SCIENTIFIC REPORTS
nature research

OPEN

An investigation of microstructural, magnetic and microwave absorption properties of multi-walled carbon nanotubes/ $Ni_{0.5}Zn_{0.5}Fe_2O_4$

Muhammad Syazwan Mustaffa[1*], Raba'ah Syahidah Azis[1,3], Nor Hapishah Abdullah[2], Ismayadi Ismail[3] & Idza Riati Ibrahim[3]

The enhancement of microwave absorbing properties in nickel zinc ferrite ($Ni_{0.5}Zn_{0.5}Fe_2O_4$) via multiwall carbon nanotubes (MWCNT) growth is studied in this research work. $Ni_{0.5}Zn_{0.5}Fe_2O_4$ was initially synthesized by mechanical alloying followed by sintering at 1200 °C and the microstructural, electromagnetic and microwave characteristics have been scrutinized thoroughly. The sintered powder was then used as a catalyst to grow MWCNT derived from chemical vapor deposition (CVD) method. The sample was mixed with epoxy resin and a hardener for preparation of composites. The composite of multi-walled carbon nanotubes/$Ni_{0.5}Zn_{0.5}Fe_2O_4$ shown a maximum reflection loss (*RL*) of −19.34 dB at the frequency and bandwidth of 8.46 GHz and 1.24 GHz for an absorber thickness of 3 mm for losses less than −10 dB. This acquired result indicates that multi-walled carbon nanotubes/$Ni_{0.5}Zn_{0.5}Fe_2O_4$ could be used as a microwave absorber application in X-band.

The high magnetic permeability, high resistivity and low eddy current loss of nickel zinc ferrite ($Ni_{0.5}Zn_{0.5}Fe_2O_4$) in the high-frequency region has made them an important candidate in soft magnetic material. One of the significant applications of this ferrite in the high frequency region is its high potential EM wave absorption properties. $Ni_{0.5}Zn_{0.5}Fe_2O_4$ exhibit good microwave absorbing performance due to its comparative properties to other ferrite[1,2]. Nevertheless, high density and poor temperature stability bound its application as a material for radar absorber in stealth aircraft and other ranges[3]. Recently, various efforts to develop microwave absorbing material in lower dimension have also been undertaken by many researchers to meet the requirements of microwave absorption applications by summarizing the structure and electronic state of 2D materials, and comprehensively overview their electromagnetic properties and response mechanisms[4–7]. As for carbon nanotubes (CNTs) which possess greater surface area and more dangling bonds causing an interfacial polarization and macroscopic quantum tunnel effect, have shown potential microwave absorbing performance[8]. Besides, the lightweight, good heat, corrosion and thermal shock resistance, higher thermal and electrical conductivity of CNTs advantage them as an auspicious candidate for advanced composite usage[9–11]. Previous research has shown that various percent of CNT introduction into soft and hard ferrite via sol-gel method, *in situ* precipitation, hydrothermal and *in situ* solvothermal has significantly improved the microwave absorption characteristics. The introduction of CNT into ferrite samples also has increased the conductivity[12–16]. In the present research work, multi-walled carbon nanotubes/$Ni_{0.5}Zn_{0.5}Fe_2O_4$ was synthesized using chemical vapour deposition (CVD) by using sintered $Ni_{0.5}Zn_{0.5}Fe_2O_4$ powder as a catalyst to investigate the impact of hybridization between magnetic and dielectric part towards the electromagnetic and microwave properties of the composite.

[1]Department of Physics, Faculty of Science, Universiti Putra Malaysia, 43400, Serdang, Selangor, Malaysia. [2]Functional Devices Laboratory, Universiti Putra Malaysia, 43400, Serdang, Selangor, Malaysia. [3]Materials Synthesis and Characterization Laboratory, Universiti Putra Malaysia, 43400, Serdang, Selangor, Malaysia. *email: mm_syazwan@upm.edu.my

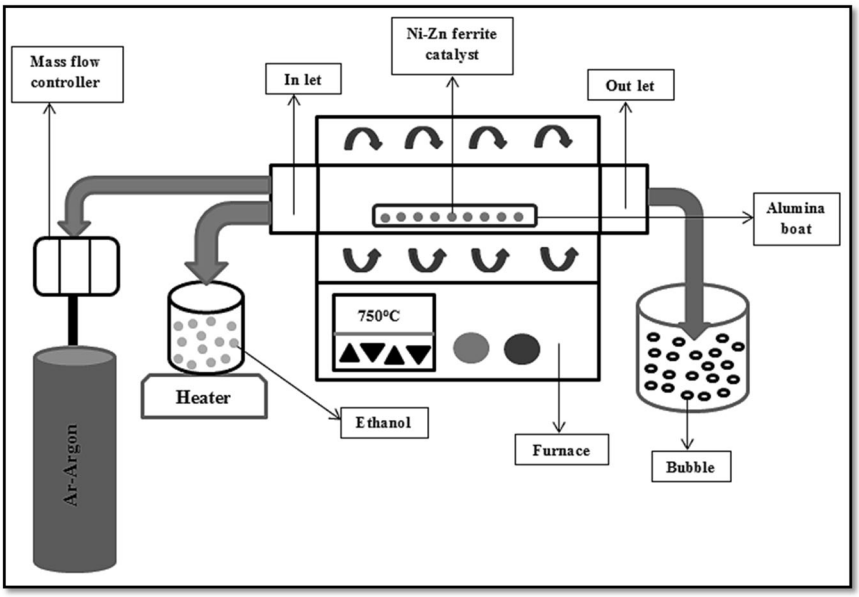

Figure 1. Schematic diagram of chemical vapor deposition (CVD).

Experimental Procedure

Preparation of $Ni_{0.5}Zn_{0.5}Fe_2O_4$. All chemicals in this work were analytical grade reagents and used as raw materials without further purification. Nickel oxide, NiO (99.99%), zinc oxide, ZnO (99.99%) and iron oxide, Fe_2O_3 (99.95%) were provided and purchased from Alfa Aesar (Ward Hill, Massachusetts, U.S.). $Ni_{0.5}Zn_{0.5}Fe_2O_4$ has been prepared using Spex8000D milling apparatus for 2 h and the milled powders have been sintered for 10 h at a temperature of 1200 °C.

Preparation of multi-walled carbon nanotubes/$Ni_{0.5}Zn_{0.5}Fe_2O_4$. Sintered powder of $Ni_{0.5}Zn_{0.5}Fe_2O_4$ was acting as a catalyst while an ethanol, C_2H_5OH (96%, Sigma Aldrich) solution as a carbon source in order to grow multiwall carbon nanotubes (MWCNT) via chemical vapor deposition (CVD) process (Fig. 1). The furnace was closed after placing an alumina boat that contained 0.6 g of $Ni_{0.5}Zn_{0.5}Fe_2O_4$ sintered powder with argon flushed at 100 sccm. Once the furnace reaches the targeted synthesis temperature at 750 °C, the evaporated ethanol solution at 100 °C temperature flowed for 30 min. After the process of flowing ethanol was completed, the furnace was left to cool down until room temperature before the sample was taken out for analysis.

Preparation of multi-walled carbon nanotubes/$Ni_{0.5}Zn_{0.5}Fe_2O_4$ composite. The composite samples were produced by blending multi-walled carbon nanotubes/$Ni_{0.5}Zn_{0.5}Fe_2O_4$ powders with an epoxy resin (Araldite 506, Sigma Aldrich) in a 60:40 weight ratio. The mixture was poured in the different rectangular-shaped sample holder (model WR 90) of 2 and 3 mm thickness and being dried overnight in room temperature.

Characterization. The phase identification was determined using X-ray diffraction, XRD (Philips X'pert Diffractometer model 7602 EA Almelo) with CuKα radiation ($\lambda = 1.5406$ Å). The surface morphology and elemental composition of the samples were observed by field emission scanning electron microscopy, FESEM (FEI Nova NanoSEM 230) fortified with an energy-dispersive X-ray, EDX (Oxford Instruments) system. Microwave and electromagnetic (EM) wave properties of the $Ni_{0.5}Zn_{0.5}Fe_2O_4$/MWCNT composites were performed via vector network analyzer, VNA (PNA N5227A) in the frequency range of 8 to 12 GHz.

Results and Discussion

Phase and microstructural analysis. Figure 2 showing the XRD pattern of multi-walled carbon nanotubes/$Ni_{0.5}Zn_{0.5}Fe_2O_4$. The appearance of the diffraction peaks at $2\theta = 28.8°$, 34.4°, 35.8°, 43.6°, 54.2°, 56.8° and 63.3° which corresponds to (220), (311), (222), (400), (422), (511) and (440) crystal planes, in consistent with the database found in the JCPDS file No. 08-0234, specify the formation of single-phase cubic of $Ni_{0.5}Zn_{0.5}Fe_2O_4$ with no extraordinary phase peaks. The observed diffraction peak appeared around $2\theta = 24.6°$ is corresponds to the graphite (002) plane of MWCNT, which confirms the retaining of MWCNT structure without any destruction[17]. The existence of graphite lattice plane in XRD pattern indicates that the MWCNT were successfully synthesized by implementing $Ni_{0.5}Zn_{0.5}Fe_2O_4$ as a catalyst to grow the MWCNT.

Figure 3 displays the FESEM image of multi-walled carbon nanotubes/$Ni_{0.5}Zn_{0.5}Fe_2O_4$. The outer diameter of MWCNTs is approximately ~50 nm. It should be noted that a huge amount of MWCNTs were deposited and dispersed almost co nsistently on the outer surface of nickel zinc ferrite particles. These surface functional groups could strongly bind to metal ions through an electrostatic attraction and assist as nucleation precursors.

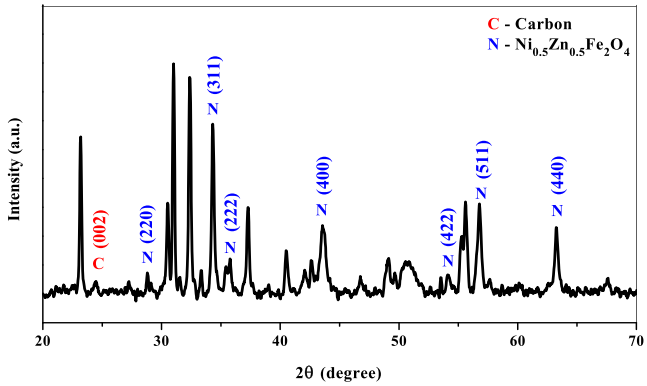

Figure 2. XRD pattern of multi-walled carbon nanotubes/$Ni_{0.5}Zn_{0.5}Fe_2O_4$.

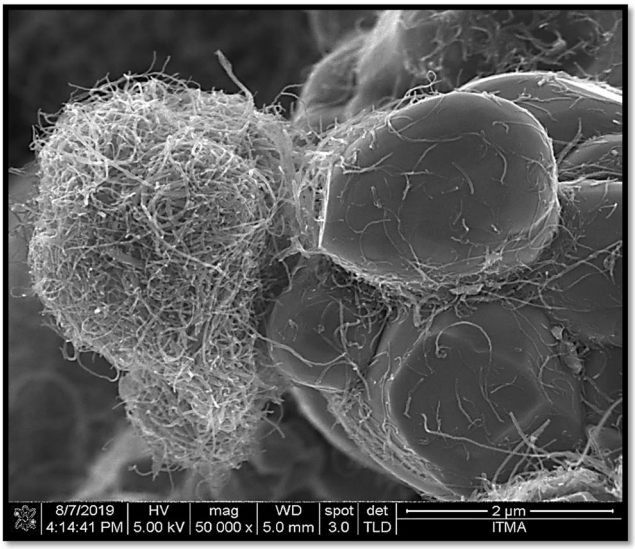

Figure 3. FESEM image of multi-walled carbon nanotubes/$Ni_{0.5}Zn_{0.5}Fe_2O_4$.

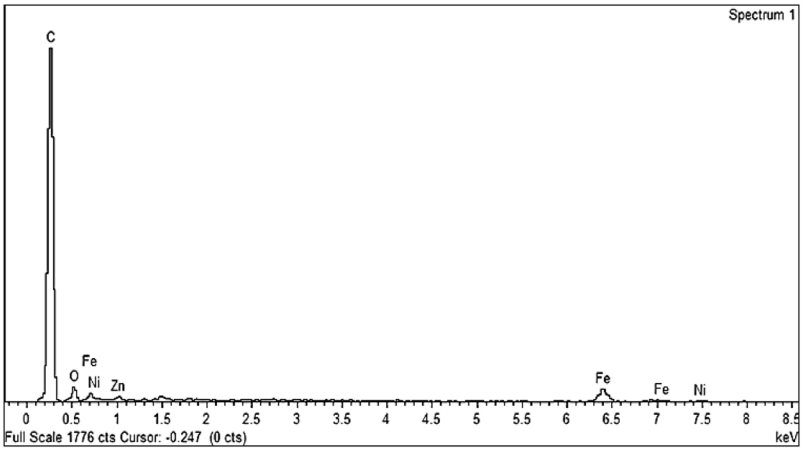

Figure 4. EDX pattern of multi-walled carbon nanotubes/$Ni_{0.5}Zn_{0.5}Fe_2O_4$.

Energy dispersive X-ray (EDX) was carried out in order to justify the chemical composition of prepared sample. The EDX spectra clearly revealed only existence of zinc (Zn), nickel (Ni), carbon (C), iron (Fe) and oxygen (O) peaks with no other contaminating constituent as can be perceived in Fig. 4.

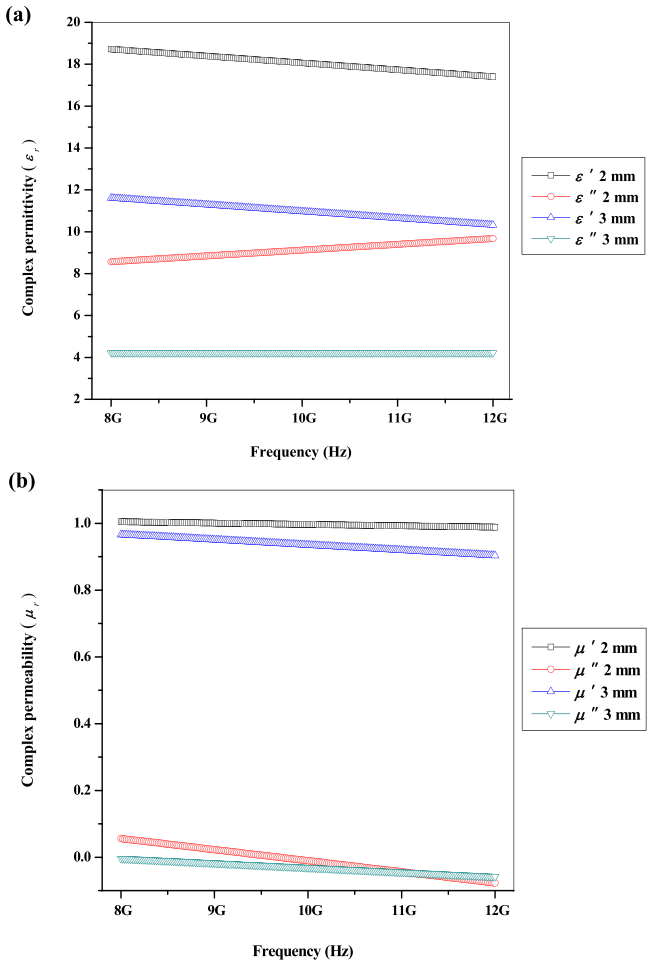

Figure 5. (**a**) Complex permittivity of multi-walled carbon nanotubes/$Ni_{0.5}Zn_{0.5}Fe_2O_4$.

Electromagnetic (EM) analysis. Microwave absorbers are characterized by their electric permittivity and magnetic permeability as exposed in Fig. 5(a,b). The permittivity is a measure of the material's effect on the electric field in the EM wave and the permeability is a measure of the material's effect on the magnetic component of the wave. The permittivity is complex and is generally written as:

$$\varepsilon_r = \varepsilon' - j\varepsilon'' \tag{1}$$

Analogous to the electric permittivity is the magnetic permeability which is written as:

$$\mu_r = \mu' - j\mu'' \tag{2}$$

The imaginary parts (μ'', ε'') denote the dissipation of magnetic and electric energies while the real parts (μ', ε') represent the storage capability of magnetic and electric energies with both of them are frequency dependent. The material's effect on the wave is entirely identified if the complex permeability and permittivity were known over a frequency range. Figure 5(a) illustrates the complex permittivity graph of multi-walled carbon nanotubes/$Ni_{0.5}Zn_{0.5}Fe_2O_4$ at different thicknesses. It can be observed that values of ε' and ε'' were about 4 to 19 with no significant changes in the whole range of frequency (8–12 GHz). The ε' values indicates a decreasing trend while the ε'' values show an increasing trend versus frequency changes which is due to the dipolar/orientation polarization mechanism[18–23]. When the EM wave from the network analyzer penetrates through the sample, it will manages to rotate and align the dipole moment with the field finds itself later colliding with another molecule and losing its alignment. At a higher thickness (3 mm), the EM energy to stimulate the dipole moment was decreased due to longer path for the EM to travel. Therefore, only slightly dipole is capable of being immobilized causing ε' and ε'' values to be reduced relative to the sample that having lower thickness (2 mm)[21–23]. In addition, the ε' and ε'' value at 2 mm thickness was higher than 3 mm thickness since it inversely proportional relation as confirmed by Eq. 3[24]:

$$\varepsilon' = \left(1 + \frac{\Delta\phi\lambda_0}{360d}\right)^2 \text{ and } \varepsilon'' = \frac{\Delta\phi\lambda_0\sqrt{\varepsilon'}}{8.686\pi d} \tag{3}$$

where ε' is real permittivity of sample, ε'' is imaginary permittivity of sample, λ_o is guided wavelength, d is sample thickness and $\Delta\phi$ is phase difference between incident and reflected waves.

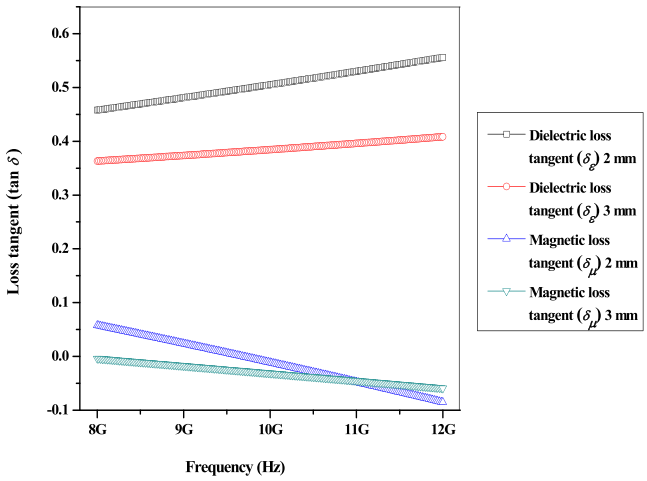

Figure 6. Dielectric and magnetic loss tangent of multi-walled carbon nanotubes/$Ni_{0.5}Zn_{0.5}Fe_2O_4$.

The complex permeability of multi-walled carbon nanotubes/$Ni_{0.5}Zn_{0.5}Fe_2O_4$ at different thicknesses is shown in Fig. 5(b). It can be found that μ' and μ'' values were around 0.9 to 1.0 and −0.5 to 0.05 with a decreasing trend from low to high frequency range. The decreasing trend values of μ' and μ'' were attributed to the relaxation of magnetization induced by domain wall displacement at lower frequency and spin rotation at upper frequency in the samples. At a lower thickness (2 mm), the EM energy to magnetize the magnetic (spin) moment was increased due to shorter route for the EM propagation. Thus, the μ' and μ'' values at 2 mm thickness were enhanced compared to sample that having higher thickness (3 mm) and can be related with the Eq. 4[25]:

$$\delta = \frac{1}{\sqrt{\pi f \mu_0 \mu_r \sigma}} \tag{4}$$

where δ is skin depth (thickness) of sample, f is the frequency, μ_0 is the permeability of free space ($4\pi \times 10^{-7}$ H/m), μ_r is the relative permeability of sample and σ is the electrical conductivity.

Figure 6 demonstrated the magnetic loss tangent (tan δ_μ) and dielectric loss tangent (tan δ_ε) of multi-walled carbon nanotubes/$Ni_{0.5}Zn_{0.5}Fe_2O_4$, respectively. The value of tan δ_ε lies within the range of 0.35 to 0.55 while tan δ_μ have an average value from −0.1 to 0.05. The tan δ_ε and tan δ_μ at 2 mm thickness have higher value than 3 mm thickness due to more energy had been attenuated with lower storing energy that infiltrate into the material as can be defined with Eq. 5[26]:

$$\tan\delta_\varepsilon = \frac{\varepsilon''}{\varepsilon'} \quad \text{and} \quad \tan\delta_\mu = \frac{\mu''}{\mu'} \tag{5}$$

where ε' is real permittivity, ε'' is imaginary permittivity, μ' is real permeability and μ'' is imaginary permeability.

The multi-walled carbon nanotubes/$Ni_{0.5}Zn_{0.5}Fe_2O_4$ composites retain a higher tan δ_ε at 8–12 GHz which implies that the EM microwave absorption is contributed by dielectric loss mechanism rather than magnetic loss mechanism[18–20].

Microwave absorption analysis. Figure 7 shows the measured *RL* of the multi-walled carbon nanotubes/$Ni_{0.5}Zn_{0.5}Fe_2O_4$ composite with difference thicknesses of 2 and 3 mm respectively in the 8–12 GHz frequency range. The multi-walled carbon nanotubes/$Ni_{0.5}Zn_{0.5}Fe_2O_4$ gained the maximum absorption loss with *RL* −19.34 dB with a bandwidth of 1.24 GHz at a frequency of 8.46 GHz on the thickness of 3 mm which manifests optimum ability of microwave absorption (Table 1). The microwave absorption at 3 mm has been perceived to be increased compared to prior thickness of 2 mm as a result of better impedance matching between dielectric and magnetic loss of a material[19–23]. In addition, the absorption peak in this sample was attributed to the existence of both dielectric and magnetic resonance at the similar frequency. Generally, the EM wave absorbing characteristics were calculated using Eqs 6 and 7[20–23,27–29]:

$$R(\text{dB}) = 20\log\left|\frac{Z_{in} - 1}{Z_{in} + 1}\right| \tag{6}$$

which Z_{in} is specified by

$$Z_{in} = \sqrt{\frac{\mu_r}{\varepsilon_r}}\tanh\left[j\frac{2\pi}{c}\sqrt{\mu_r\varepsilon_r}ft\right] \tag{7}$$

where Z_{in} denotes an absorber input impedance, c is the speed of light, t is thickness of sample, f is microwave frequency, ε_r is relative complex permittivity and μ_r is relative complex permeability. The resonance frequency, f_m

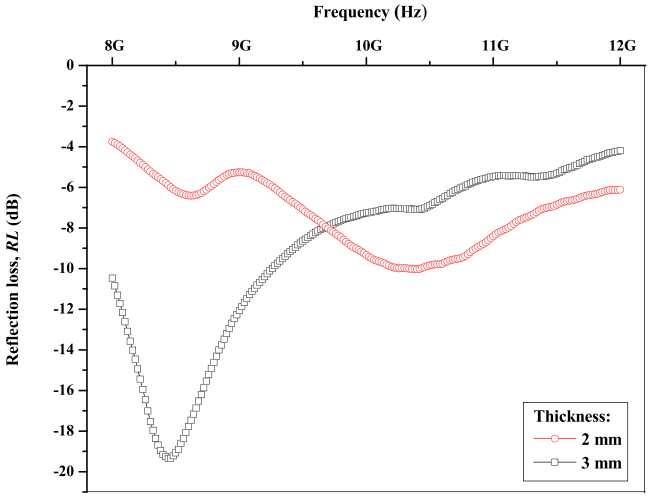

Figure 7. Reflection loss (*RL*) of multi-walled carbon nanotubes/$Ni_{0.5}Zn_{0.5}Fe_2O_4$.

Thickness of sample, *d* (mm)	Reflection loss, *RL* (dB)	Resonance frequency, f_m (GHz)	Bandwidth (GHz) (*RL* < −10 dB)
2	**10.03**	**10.40**	**0.08**
3	**19.34**	**8.46**	**1.24**

Table 1. EM wave absorption properties of multi-walled carbon nanotubes/$Ni_{0.5}Zn_{0.5}Fe_2O_4$.

was discovered to deflect towards lower frequency as the thickness of the sample was increased due to indirectly proportional relation as agreed to the Eq. 8[19–23,29,30]:

$$f_m = \frac{c}{2\pi\mu'' t} \tag{8}$$

where μ'' is an imaginary part of permeability, f_m is resonance frequency with maximum *RL*, *c* is velocity of light and t is thickness of sample.

Conclusion

Multi-walled carbon nanotubes/$Ni_{0.5}Zn_{0.5}Fe_2O_4$ was successfully fabricated by chemical vapour deposition (CVD) technique. The reflection loss peak exhibited the characteristics of a maximum loss of −19.34 dB at a frequency of 8.46 GHz, with a bandwidth of 1.24 GHz for losses less than −10 dB when the thickness of the sample was 3 mm due to the good compatibility of dielectric and magnetic properties in the sample. As a result, multi-walled carbon nanotubes/$Ni_{0.5}Zn_{0.5}Fe_2O_4$ samples have the characteristics as a suitable candidate for microwave absorber applications.

Received: 11 September 2019; Accepted: 8 October 2019;
Published online: 29 October 2019

References

1. Cho, S. B., Kang, D. H. & Oh, J. H. Relationship between magnetic properties and microwave-absorbing characteristics of NiZnCo ferrite composites. *Journal of Materials Science* **31**(17), 4719–4722 (1996).
2. Verma, A. & Dube, D. C. Processing of Nickel–Zinc Ferrites Via the Citrate Precursor Route for High-Frequency Applications. *Journal of The American Ceramic Society* **88**(3), 519–523 (2005).
3. Gang, C. X., Ying, Y. & Peng, C. J. Recent Progress in Electromagnetic Wave Absorbers. *Journal of Inorganic Material* **26**(5), 449–457 (2011).
4. M. S., Cao *et al*. Electronic Structure and Electromagnetic Properties for 2D Electromagnetic Functional Materials in Gigahertz Frequency. *Annalen der Physik*, 1800390 (2019).
5. Zhang, M., Wang, X. X., Cao, W. Q., Yuan, J. & Cao, M. S. Electromagnetic Functions of Patterned 2D Materials for Micro–Nano Devices Covering GHz, THz, and Optical Frequency. *Advanced Optical Materials*, 1900689 (2019).
6. Wen, B. *et al*. Reduced Graphene Oxides: Light-Weight and HighEfficiency Electromagnetic Interference Shielding at Elevated Temperatures. *Advanced Materials* **26**, 3484–3489 (2014).
7. M. S. Cao *et al*. Electromagnetic Response and Energy Conversion for Functions and Devices in Low-Dimensional Materials. *Advanced Functional Materials*, 1807398 (2019).
8. Thomassin, J. M., Huynen, I., Jerome, R. & Detrembleur, C. Functionalized polypropylenes as efficient dispersing agents for carbon nanotubes in a polypropylene matrix; application to electromagnetic interference (EMI) absorber materials. *Polymer* **51**(6), 115–121 (2010).
9. LeRoy, B. J., Lemay, S. G., Kong, J. & Dekker, C. Erratum: "Scanning tunneling spectroscopy of suspended single-wall carbon nanotubes". *Applied Physics Letters* **85**(18), 4956–4958 (2004).

10. Baughman, R. H., Zakhidov, A. A. & de Heer, W. A. Carbon Nanotubes-the Route Toward Applications. *Science. Science* **297**(5582), 787–792 (2002).
11. Iijima, S. Helical microtubules of graphitic carbon. *Nature* **354**(7), 56–58 (1991).
12. Jiang, L. & Gao, L. Carbon Nanotubes—Magnetite Nanocomposites from Solvothermal Processes: Formation, Characterization, and Enhanced Electrical Properties. *Chemistry of Materials* **15**(14), 2848–2853 (2003).
13. Liu, Y. & Gao, L. A study of the electrical properties of carbon nanotube-$NiFe_2O_4$ composites: Effect of the surface treatment of the carbon nanotubes. *Carbon* **43**(1), 47–52 (2005).
14. Cao, H. *et al*. A highly coercive carbon nanotube coated with $Ni_{0.5}Zn_{0.5}Fe_2O_4$ nanocrystals synthesized by chemical precipitation–hydrothermal process. *Journal of Solid State Chemistry* **180**(11), 3218–3223 (2007).
15. Ghasemi, A. Remarkable influence of carbon nanotubes on microwave absorption characteristics of strontium ferrite/CNT nanocomposites. *Journal of Magnetism and Magnetic Materials* **323**(23), 3133–3137 (2011).
16. Akhtar, M. N., Yahya, N., Koziol, K. & Nasir, N. Synthesis and characterizations of $Ni_{0.8}Zn_{0.2}Fe_2O_4$-MWCNTs composites for their application in sea bed logging. *Ceramics International* **37**(8), 3237–3245 (2011).
17. Ghasemi, A. The role of multi-walled carbon nanotubes on the magnetic and reflection loss characteristics of substituted strontium ferrite nanoparticles. *Journal of Magnetism and Magnetic Materials* **330**, 163–168 (2013).
18. Song, W.-L., Cao, M.-S., Hou, Z.-L., Fang, X.-Y. & Shi, X.-L. High dielectric loss and its monotonic dependence of conducting-dominated multiwalled carbon nanotubes/silica nanocomposite on temperature ranging from 373 to 873 K in *X*-band. *Applied Physics Letters* **94**, 233110 (2009).
19. Cao, M. S., Song, W. L., Hou, Z. L., Wen, B. & Yuan, J. The effects of temperature and frequency on the dielectric properties, electromagnetic interference shielding and microwave-absorption of short carbon fiber/silica composites. *Carbon* **48**, 788–796 (2010).
20. Wen, B. *et al*. Temperature dependent microwave attenuation behavior for carbon-nanotube/silica composites. *Carbon* **65**, 124–139 (2013).
21. M. Cao *et al*. Thermally Driven Transport and Relaxation Switching Self-Powered Electromagnetic Energy Conversion. *Small*, 1800987 (2018).
22. He, P. *et al*. Atomic Layer Tailoring Titanium Carbide MXene to Tune Transport and Polarization for Utilization of Electromagnetic Energy beyond Solar and Chemical Energy. *ACS Applied Materials & Interfaces* **11**(13), 12535–12543 (2019).
23. Cao, W. Q., Wang, X. X., Yuan, J., Wang, W. Z. & Cao, M. S. Temperature dependent microwave absorption of ultrathin graphene composites. *Journal of Materials Chemistry C* **3**, 10017 (2015).
24. Kim, J. H., Kim, K. B. & Noh, S. H. New density independent model for measurement of grain moisture content using microwave techniques. *Journal of Electronics Engineering and Information Science* **2**(4), 72–78 (1997).
25. Idris, F. M. *et al*. Recent developments of smart electromagnetic absorbers based polymer-composites at gigahertz frequencies. *Journal of Magnetism and Magnetic Materials* **405**, 197–208 (2016).
26. Cheng, E. M. *et al*. The use of dielectric mixture equations to analyze the dielectric properties of a mixture of rubber tire dust and rice husks in a microwave absorber. Progress In Electromagnetics. *Research* **129**, 559–578 (2012).
27. Syazwan, M. M. *et al*. Co–Ti and Mn–Ti substituted barium ferrite for electromagnetic property tuning and enhanced microwave absorption synthesized via mechanical alloying. *Journal of the Australian Ceramic Society* **53**(2), 465–474 (2017).
28. Syazwan, M. M. *et al*. Enhancing absorption properties of Mg–Ti substituted barium hexaferrite nanocomposite through the addition of MWCNT. *Journal of Materials Science: Materials in Electronics* **28**(12), 8429–8436 (2017).
29. Hapishah, A. N., Syazwan, M. M. & Hamidon, M. N. Synthesis and characterization of magnetic and microwave absorbing properties in polycrystalline cobalt zinc ferrite ($Co_{0.5}Zn_{0.5}Fe_2O_4$) composite. *Journal of Materials Science: Materials in Electronics* **29**(24), 20573–20579 (2018).
30. Liu, L. D., Duan, Y. P., Ma, L. X., Liu, S. H. & Yu, Z. Microwave absorption properties of a wave-absorbing coating employing carbonyl-iron powder and carbon black. *Applied Surface Science* **257**(3), 842–846 (2010).

Acknowledgements

The authors are grateful to Universiti Putra Malaysia Grants (UPM/700-1-2/GPPI/2017/954160, GP-IPS 9580600, GP/2018/9628400) and MOE/FRGS 5524942 for the funds. The authors also thank to Material Synthesis Characterization Laboratory, Institute of Advance Technology (ITMA), Universiti Putra Malaysia for the CVD facilities.

Author contributions

M.S.M. and N.H.A. designed, conducted the experiments and analyzed data. R.S.A., I.I. and I.R.I. supervised the experimental work. All authors contributed to the discussion and writing of the manuscript.

Competing interests

The authors declare no competing interests.

Additional information

Correspondence and requests for materials should be addressed to M.S.M.

Reprints and permissions information is available at www.nature.com/reprints.

Publisher's note Springer Nature remains neutral with regard to jurisdictional claims in published maps and institutional affiliations.